Performance Evaluation of an Over-Driven LED for High-Speed Schlieren Imaging

S. Wilson[1], G. Gustafson[1], D. Lincoln[1], K. Murari[2] and C. Johansen[1]
(1) Mechanical Engineering Department, University of Calgary, Canada
(2) Electrical and Computer Engineering Department, University of Calgary, Canada

Abstract
A quantitative comparison of an over driven light emitting diode (LED) and a high intensity discharge lamp (HID) as illumination sources for high-speed schlieren imaging is presented. A custom pulser circuit utilizing a new and improved driver circuit was developed to over-drive the LED by a factor of ten while simultaneously reducing pulse widths to sub-microsecond durations. The LED system has been developed as a simple and inexpensive alternative light source to discharge lamps and pulsed laser systems, which are typical for high-speed schlieren imaging. Image quality of a decaying spherical shock wave, produced from the unsteady release of an under-expanded helium jet, is analyzed to assess comparative performance. The effects of framing rate, camera exposure time, and pulse duration on image quality were assessed and compared for the novel LED and a high intensity discharge lamp. Framing rates of 10,000 fps and 50,000 fps and exposure times of 1 μs and 10 μs were tested. Image quality was assessed qualitatively through side-by-side comparisons of fluid dynamic features such as the resolution of shock waves, compression waves, and shear layers. Quantitative analysis was performed through the comparison of the signal-to-noise ratio at the various conditions. LED performance was found to be superior when imaging fast events and inferior when imaging slower events. Results and potential system improvements indicate that the LED system is ideal for low-cost, high-speed flow imaging.

Keywords schlieren imaging - light emitting diode (LED) - high intensity discharge (HID) lamp - shock propagation

1 Introduction
Recent advances in digital camera technology have allowed for the visualization of high-speed, unsteady flows with high spatial and temporal resolution at a reasonable cost. This has enabled new experimental work to be performed on applications related to explosions and hypersonic aerodynamics using high-speed schlieren photography. For example, Mizukaki *et al.* (2013) performed background oriented schlieren (BOS) measurements of an open-air detonation of a C-4 explosive [1]. The optical displacement of natural obstacles in the background such as trees and grass were used to extract the shock wave overpressure during the explosion. In these experiments, a Phantom v10 (Vision Research Inc., NJ) camera, providing 800 x 600 pixels at 10,000 fps, was used. In an explosion chamber, Ciccarelli *et al.,* (2013) used schlieren photography to study the flame acceleration process responsible for deflagration-to-detonation transition (DDT) [2]. A FASTCAM SA5 (Photron, CA) camera was used, which provides 1024 x 744 pixels at 10,000 fps. Saravanan *et al.,* (2011) used a high-speed schlieren system in a shock tunnel to study the hypersonic flow around a missile-shaped body [3]. A Phantom v7.2 (Vision Research Inc., NJ) camera was used to provide 450 x 450 pixels at a framing rate of 10,000 fps.

Since the time scales associated with these fluid dynamic events are short, one of the key requirements is to effectively freeze the motion of the flow by decreasing the total camera exposure time (duration for which the camera collects photons from the field of view) during each frame [4]. With continuous light sources, such as arc lamps and continuous wave lasers, the exposure duration is completely controlled by the camera's electronic shutter settings. At the time of this writing, many high-speed digital cameras are limited to electronic shutter times on the order of one microsecond. Faster shutter times are restricted by the International Traffic in Arms Regulations (ITAR) [5]. Therefore, a requirement for the continuous light source is to provide adequate light for the schlieren system as camera shutter time is decreased. Arc lamps, such as high intensity discharge (HID) lamps, are considered to be of low-cost and can provide adequate lighting at moderately low shutter times (~1 μs). There are several examples in the literature of high-speed schlieren experiments using such continuous light sources [2, 6, 7]. Without reducing the time duration of the light source, the maximum velocity that can be imaged with acceptable blur is limited by the camera's electronic shutter.

Spark gaps, pulsed lasers and light emitting diodes (LEDs) are typical light sources used with schlieren systems that can be pulsed to reduce the total exposure time during each frame. The exposure time is then effectively independent of the shutter time of the camera, as long as its duration is longer than that of the pulse and timed such that the sensor is exposed for the entire pulse duration. Although the spark gap has a very short and bright duration pulse, it is costly and typically only runs in a single-shot mode. Pulsed lasers and LEDs provide variable short duration pulses at high repetition rates and are relatively low in cost. There are several examples of LED and pulsed laser light sources used for schlieren applications reported in the literature [8, 9, 10]. A cost comparison was conducted for three different typical low-cost light source options. The cost of the CBT-120 LED system, which was constructed in this work, is approximately $125 USD based on 2012 prices. This is approximately one third the cost of GE D2S Xenon HID Bulb with 50W DC Ballast (XVD2) used in this work for comparison, and one ninth the cost of a common Diode Laser (905D3S3J09) with LDP-V 50-100 V3 Pulser [11, 12, 13, 14]. Light source costs are highlighted since one of the motivators for this work is to decrease the cost associated with high-speed imaging.

In an effort to improve LED performance for flow visualization applications, Willert *et al.,* (2010) developed a pulser circuit to over-drive a commercial LED [15]. A basic schematic for a circuit used to drive the Luminus CBT-120G LED is shown on the left of Fig. 1. Energy stored in a large capacitor is discharged through the LED repetitively to produce a series of short duration pulses. When operating at a low duty cycle (e.g. 0.1%), the capacitor can recharge between pulses, allowing the system to run indefinitely. In their work, the current handling capacities of the LED at various pulse durations were published for this low duty cycle. It was found that the LED could operate at a current load of 200 amperes for durations of less than 2 µs. This corresponds to more than ten times the current rating specified by the manufacturer. As a result, light output increased by 550% relative to baseline levels. In another work, it was demonstrated that the LED could be applied to high-speed schlieren applications [16]. With a rapid rise and fall time of light output, and the well-defined shape of the light emitting surface, the LED could be used to produce clear images of the unsteady flow of an under-expanded free jet impinging on a solid surface. By operating in a “burst mode”, it was found that the duty cycle could be increased to 25% without damaging the system. However, in burst mode the capacitors discharge too rapidly to be recharged and the capacitance of the circuit becomes a limiting factor in regards to circuit operation.

Although the novel LED system was demonstrated for both particle image velocimetry (PIV) and schlieren applications, its performance has not been compared to a competing light source and assessment based on a real fluid dynamic problem was limited. As a result, the main objective of this work is to quantitatively and qualitatively compare LED and HID light sources used for a typical high-speed fluid dynamic problem. Here, schlieren images of unsteady spherical shock wave propagation produced from a high-pressure helium jet release are analyzed. The HID and LED are selected as they represent the two least expensive light source options that are common for high-speed schlieren imaging. Additionally, the HID light source was chosen as a basis for comparison based on the use of similar arc lamps in several recent high-speed schlieren imaging applications [2, 6, 7, 17]. Image quality is qualitatively assessed through side-by-side comparisons of fluid dynamic features, as well as quantitatively assessed through the analysis of signal-to-noise ratio (SNR). A minimum of 5 tests were conducted for each combination of exposure time and frame rate. Only those images where the lead shock is crossing the field of view were used for comparison, approximately 5 frames for each test at 10 000 fps and 25 frames at 50 000 fps.

2 LED Pulser Circuit Characterization

In this work, a pulser circuit designed to repetitively over-drive a CBT-120 green LED was constructed. The design was based on information published in the literature and from private communication with Christian Willert [15, 16, 18]. Private communications and an initial analysis using Multisim simulation software (National Instruments, TX) indicated that the main performance penalties that occur in the Willert circuit are from component parasitic losses [19]. It was determined that performance could be greatly improved if wide, short traces were used on a compact printed circuit board (PCB) design. In addition, it was expected that the low ohmic resistance and reduced parasitics associated with PCBs would limit resonant current harmonics. Although also compact in design, the original Willert pulser circuit was constructed manually on a protoboard [18]. Buchmann *et al.* (2012) presented a similar modified version of the Willert circuit utilizing wide, short traces on a PCB [20].

In addition to being constructed on a PCB, several modifications were made to the design. Figure 1 shows a comparison between the original Willert circuit (left) and the modified circuit developed in the current study (right) including a list of the components used in both designs. The main difference in the modified circuit was to move the sense resister, R_{SENSE}, to the drain of the MOSFET and connect the source to ground. Thus, as the MOSFET turns on and the current increases, only the drain to source voltage (V_{DS}) reduces and the gate to source voltage (V_{GS}) of the device remains constant. Based on the operating region, MOSFET current depends on either $(V_{GS}\text{-}V_T)\times V_{DS}$ or $(V_{GS}\text{-}V_T)^2$ where V_T is the threshold voltage. Thus, the modified design allows the maximum current for a given driver supply voltage, V_{GATE}. Two capacitors in parallel were used as opposed to one, which increases overall capacitance while decreasing the electronic series resistance (ESR) of the capacitors. A zero recovery time SiC Schottky diode was added to minimize transient current oscillations. The PCB was laid out with short and wide traces and used surface mount components wherever possible to reduce parasitics and improve thermal performance. Since the circuit was designed for single burst operation without recharging the capacitors, the current limiting R_1 resistor from the original Willert circuit was removed. R_{SENSE} was reduced from 0.02 Ω to 0.005 Ω to increase the current throughput. This, along with the placement of R_{SENSE}, required the usage of a sensitive differential voltage measurement to calculate the current.

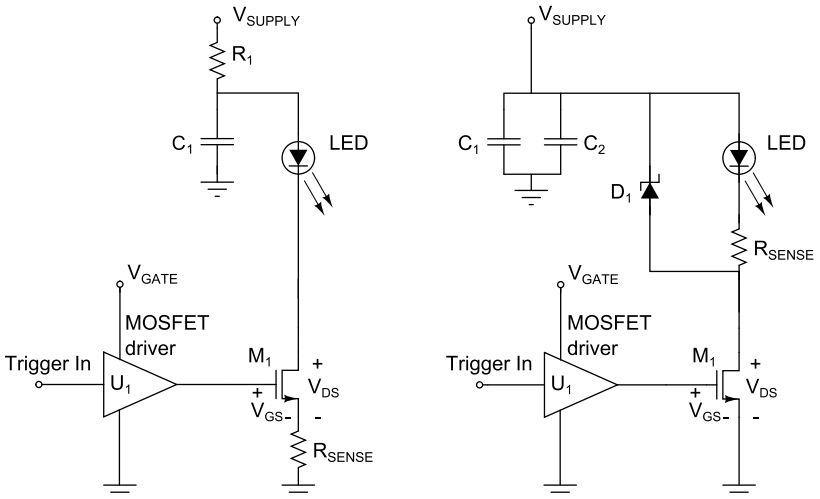

Component	Willert *et al.,* 2012	Modified Design
C_1	~1000 µF electrolytic	680 µF electrolytic
C_2	N/A	680 µF electrolytic
D_1	N/A	IDH20G65C5 Schottky Diode
LED	CBT-120 Green LED	CBT-120 Green LED
U_1	UCC37322P MOSFET driver	UCC37322P MOSFET driver
M_1	IRFB3206GPbF MOSFET	IRFB3206GPbF MOSFET
R_1	1 Ω	N/A
R_{SENSE}	0.02 Ω	0.005 Ω FCSL110R005FERCT

Fig. 1 Circuit published in Willert *et al.* 2012 (left) and modified pulser circuit for experiments in this work (right)

Important for the characterization of the modified circuit is the relationship between the supply voltage and the drive current. Independent variable DC power supplies were used to power the circuit and the MOSFET driver. V_{GATE} was fixed at 8 V and V_{SUPPLY} was varied to change the pulse current, which was monitored by measuring the voltage drop across R_{SENSE}. Data were recorded on an MSO-X 3024A oscilloscope (Agilent, CA) and processed using MATLAB (Mathworks, MA). Representative data showing the trigger in, the calculated LED current and the output of a DET02AFC photodiode (Thorlabs, NJ) monitoring the relative light output is shown in Figure 2. This data corresponds to a 1-µs-duration pulse and a supply voltage of 18.5 V. The ~125-ns delay between the trigger and the start of the current is due to the MOSFET driver latency [21]. Negative currents were not expected since the LED blocks reverse

currents unless the diode enters the breakdown region and the Schottky diode prevents a reverse voltage large enough to cause LED breakdown. Thus, the current oscillations seen after turnoff are likely due to parasitics in the oscilloscope probes. This is borne out by the clean LED response. The photodiode bandwidth is in the GHz range and the rise and fall times seen in the response are limited by the LED. Approximately 50 tests were run with a 1 µs pulse duration and a 50 pulse train to demonstrate repeatability and no adverse effects on the LED performance were detected. It is expected that the CBT-120 LED could be further over-driven at sub-microsecond pulse durations.

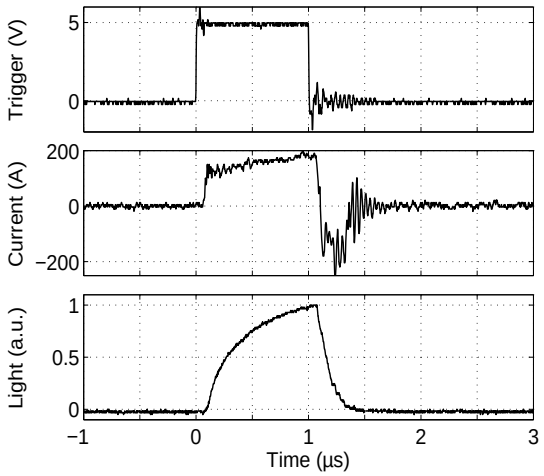

Fig. 2 Circuit response to trigger input for a 1 µs, 200 A pulse with relative LED response in arbitrary units (a.u.)

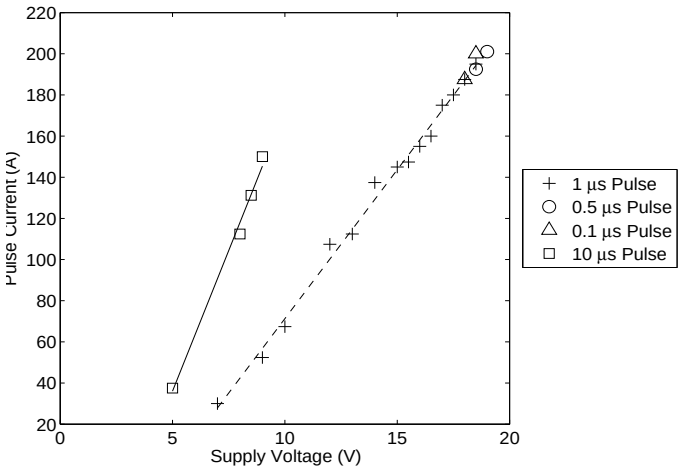

Fig. 3 Current response of modified circuit with LED to varying supply voltages for different pulse durations

Figure 3 shows effect of supply voltage and pulse duration on the measured peak pulse current. The observed linear relationship indicates that a nearly constant pulse current can be maintained, independent of pulse duration, as long as the supply voltage is kept constant. A slight increase in current across the pulse can be seen, this is due to the semiconductive nature of the LED causing resistance to be reduced as the temperature increases allowing a higher current for a constant supply voltage. However, it was found that pulse durations exceeding 1 µs required reduced supply voltages. This is because quasi-steady state operation occurs during these relatively long pulses, which reduces the voltage requirement for a given current output.

3 Fluid Dynamic Experimental Setup

To assess the performance of the light source, a high-speed fluid dynamics experiment was performed and imaged using a FASTCAM SA4 (Photron, CA) high-speed digital camera as part of a single-pass, *z*-type schlieren system. As shown in Figure 4, both the pulsed LED and continuous Xenon HID served as light sources in this optical arrangement.

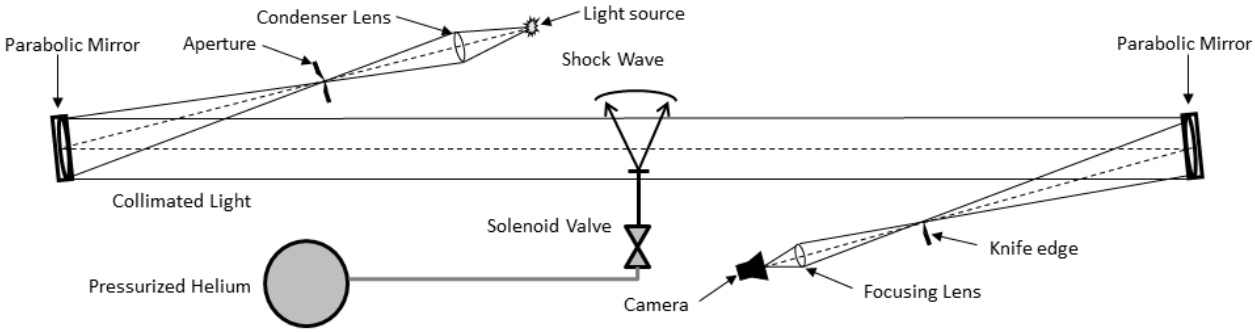

Fig. 4 Schematic of schlieren setup with the unsteady helium jet release apparatus.

In the schlieren system, light was passed through a condenser lens before reflecting off of a 20.3 cm diameter parabolic mirror. Collimated light was then directed past the jet release apparatus before reflecting off of the second

parabolic mirror. At the focal point, refracted light from density gradients in the flow was blocked (or cut-off) by a knife edge. The resultant image was then captured by the high-speed camera coupled with a 300 mm lens (Nikon, NY). The parabolic mirrors were placed 7.32 m (24 feet) apart, with the first mirror one focal length (3.05 m) from the light source, and second mirror positioned one focal length from the knife edge. Image quality is affected by the light source size, brightness and shape. In particular, brightness affects the minimum discernible contrast in a schlieren system, which then determines the minimum visible density gradient for a given knife edge placement [22]. In this study the knife edge position was adjusted such that the mean pixel value across the entire frame of view was 50% of that when the knife edge is not in place for an undisturbed flow field. This was found to provide adequate sensitivity and provided a consistent method for comparison between light sources and exposure times. An excellent review of schlieren photography including setup and applications is given by Gary Settles [22].

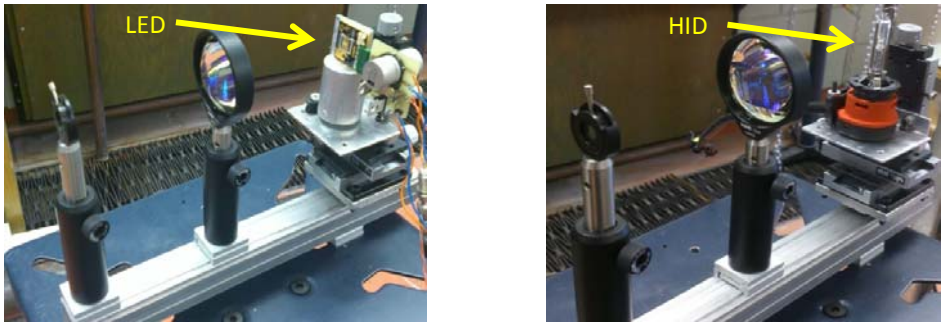

Fig. 5 Pictures of mounted LED (left) and HID (right).

Figure 5 shows photographs of the LED and HID installed on an optical rail with a condenser lens and aperture. The position of the condenser lens was selected to optimize image brightness while maintaining signal uniformity across the image. The aperture aided in maintaining uniform light distribution by only transmitting the center portion of the beam. The aperture was fixed at a diameter of 12 mm (0.472 in) for all tests conducted. A protective enclosure was finally installed over each of the light sources, with a hole positioned at the aperture.
In the experiment, a propagating spherical shock wave was produced from the unsteady release of an under-expanded helium jet. The high speed of sound in helium allows for fast expansion of the gas, producing stronger shock waves for a given initial pressure. Helium was also used because it has very low density compared to air, resulting in large density gradients in the shear layer of the jet. This is advantageous since the signal in a schlieren image is proportional to the magnitude of the density gradient.

To initiate the experiment, helium pressurized at 13.8 bar was filled into a 6.35 mm diameter and 122.5 mm (5 inch) long stainless steel pipe. The end of the pipe was initially sealed by a 13.5 mm diameter and approximately 0.02 mm thick aluminum diaphragm. The diaphragm material was selected for its reflective surface and the dimensions were chosen so that it could rupture at relatively low pressures. The filling time and rupture pressure (7.6 bar) were controlled by an MS 15E5 solenoid valve (E.MC Machinery, Ningbo, China). A red diode laser was reflected off the diaphragm onto a PDA36A amplified Si Photodiode (Thorlabs, NJ). The reflection is interrupted as the diaphragm ruptures, and the resulting falling edge in the photodiode output was used to trigger the camera and the LED pulse train. In tests where the continuous HID was used as the light source, the trigger signal was sent only to the camera. Side and front views of the jet release apparatus are shown in Figure 6.

Fig. 6 Side view (left) and front view (right) of unsteady jet release apparatus.

4 Qualitative Image Assessment

Figure 7 shows a qualitative comparison of schlieren images obtained using HID and LED light sources at various exposure times. The framing rate and resolution are 10 kfps and 960 x 400 pixels, respectively. The magnification in the image is approximately 0.21 mm/pixel. The overall brightness of each image has been artificially scaled such that the background intensity is the same for all of the cases. The jet release apparatus appears as a black shadow on the left side of each image whereas the parabolic mirror appears as a dark curved surface.

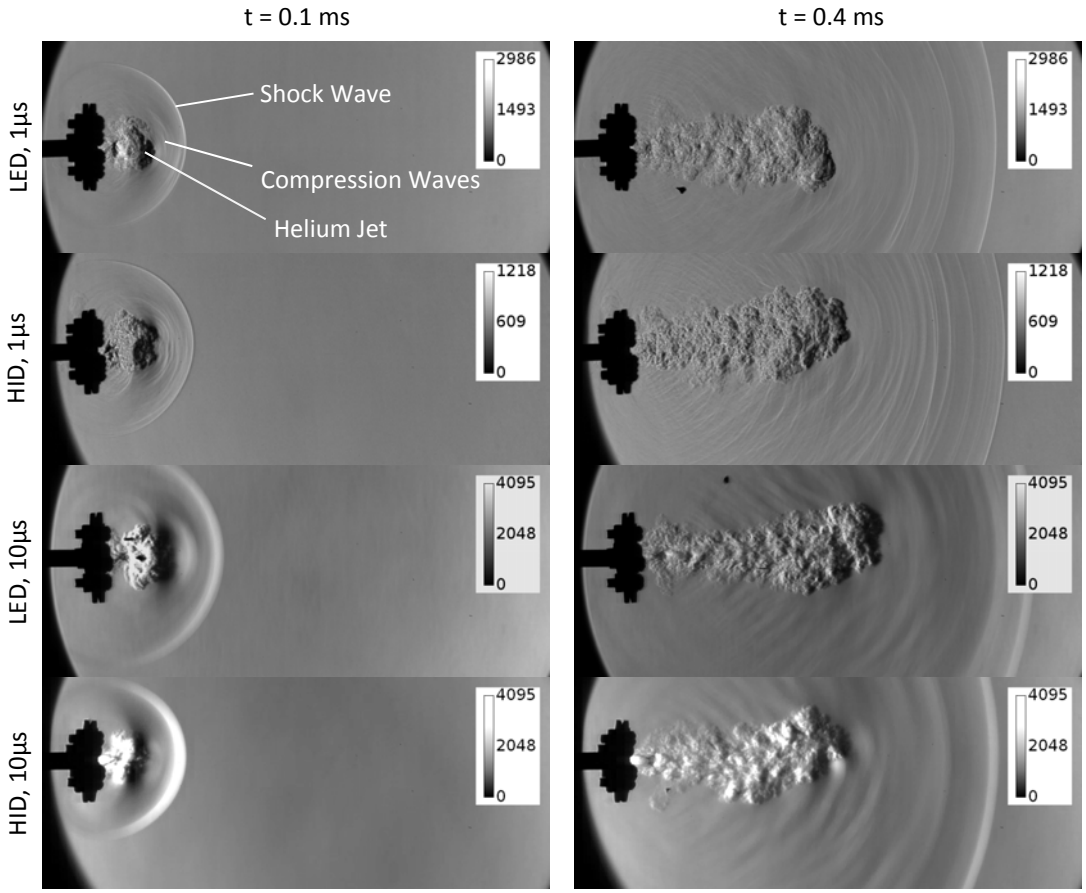

Fig. 7 Effect of pulse width and light source on qualitative schlieren image quality (10 kfps).

After the diaphragm ruptures, the high pressure helium expands into the surrounding low-pressure air. This sudden expansion causes a spherical shockwave to form at the pipe exit. At ambient conditions, the Mach 1.15 spherical shock wave travels at approximately 396 m/s. The spherical wave decayed to a weak compression wave (~Mach 1)

near the end of the field of view. As the shock wave propagates, its surface area grows causing a decrease in shock strength. As a result, the shock wave velocity, overpressure, and density ratio decrease with increasing distance. This is one of the causes for the wave to appear dimmer in the later images. As the helium interacts with the surrounding air, a strong shear layer is formed. Instabilities in the shear layer cause small-scale turbulence structures to form and become visible in the images. Note that the helium jet travels at much lower speeds than that of the lead shock wave. Furthermore, the jet trajectory is sensitive to the nature of the diaphragm rupture. Asymmetric rupture can cause the jet to be directed away from the horizontal plane, as evident in the images. Small-amplitude pressure waves are observed between the shear layer and lead shock. These propagate at roughly the local speed of sound (344 m/s). Differences in the position of the lead shock observed in the images are mainly due to small variances in the delay time between camera triggering and diaphragm rupture.

At 1 μs exposure times, both the HID and LED images show similar levels of sharpness and detail. Although subtle, the LED shows more information in the jet at t = 0.1 ms while showing less information in the jet at t = 0.4 ms, compared to the HID. This can be seen by the discernable turbulence structures within the helium jet and distinct compression waves for the LED which are not visible for the HID at 0.1 ms. It is possible that the superior spatial uniformity characteristics associated with the LED have contributed to the improved image quality that is observed in the LED images. At 10 μs exposure times, the lead shock wave and interior compression waves appear to be significantly blurred for both light sources, as indicated by the large thickness of the waves. As expected, the jet shear layer does not appear as affected by blurring as it propagates at lower velocities. Also apparent in the images is the varying brightness of the flow structures. At t = 0.1 ms, structures in the image corresponding to the LED (10 μs) tests appear to be of comparable brightness as those corresponding to the LED (1 μs) and HID (1 μs) tests. However, the structures corresponding to the HID at a 10 μs exposure are significantly brighter than all other tests. This is because the HID operates at a constant brightness independent of exposure time, whereas the limited energy stored in the capacitors for the LED cause a fewer overall number of photons to be emitted over the long run. Furthermore, it is evident that the LED capacitors have drained substantially at t = 0.4 ms when operating at a 10 μs pulse duration at 10 kfps. This results in an overall dim image, although the structures can still be discerned. It is clear that the HID (10 μs) is able to produce a bright, relatively sharp image of the slow moving jet shear layer at t = 0.4 ms. Figure 8 shows the measured (markers) and interpolated (lines) temporal response of the background image intensity for each of the runs. Note that the background intensity decays rapidly when the LED is operated with a 10 μs exposure. Note that t = 0.1 ms and 0.4 ms in Fig. 7 correspond to frames 1 and 4 in Fig. 8.

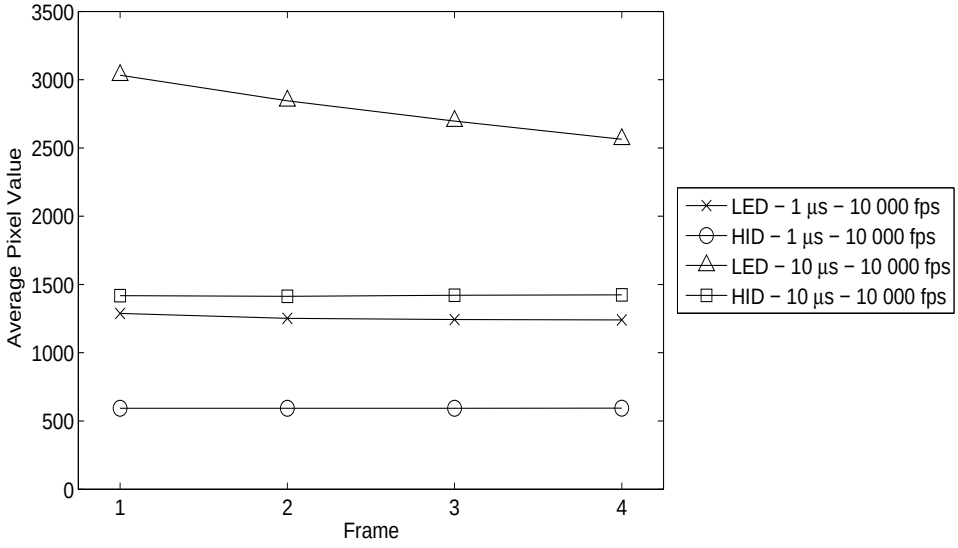

Fig. 8 Background image intensity corresponding to HID and LED tests at various conditions.

5 Quantitative Assessment

To better quantify the differences that are observed qualitatively, a quantitative analysis of SNR was performed. As a reference, the ISO 12232 standard for determining image quality suggests that an SNR value of 10 corresponds to

acceptable image quality, while an SNR value of 40 corresponds to excellent image quality [23]. The images were background subtracted and corrected for mean background non-uniformity. As shown in Fig. 9, a second order polynomial was fitted to the signal values along the image centerline downstream of the lead shock wave in the original image and subtracted to correct for any mean non-uniformity in the background. The signal value for the image was determined from the peak value associated with the lead shock wave from the corrected signal. The noise was approximated from a spatial standard deviation of the corrected signal upstream of the shock wave to the right side of the frame.

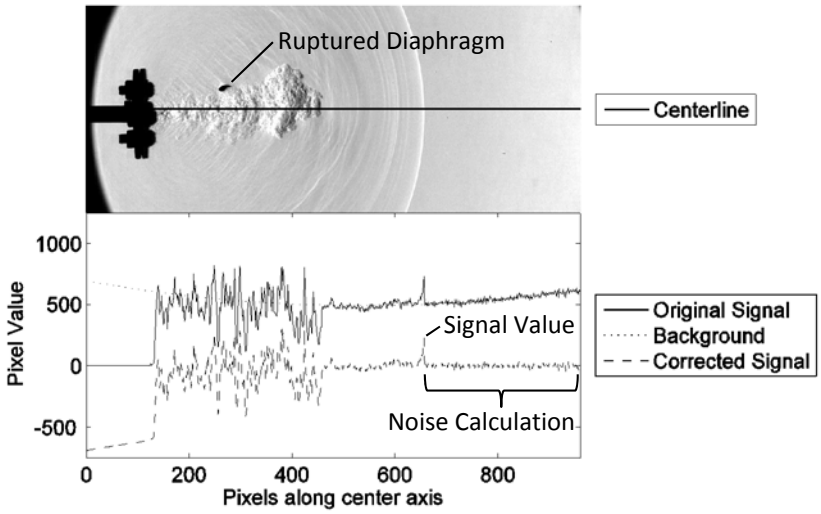

Fig. 9 Image processing of centerline signal extracted from the schlieren images (LED, 10kfps, 1µs).

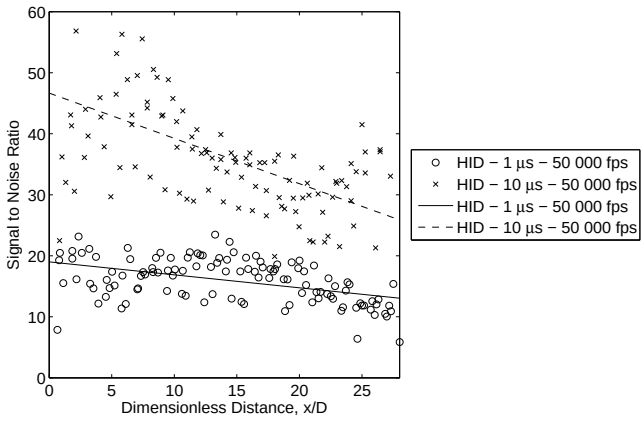

Fig. 10 Signal to Noise Ratio for HID versus distance from pipe exit non-dimensionalized by pipe diameter at 50 kfps for various exposure times.

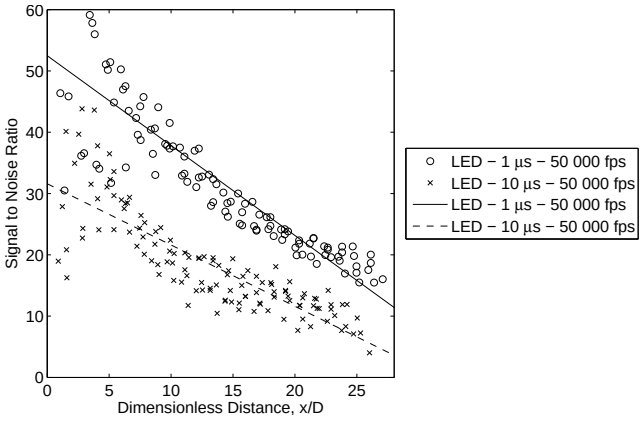

Fig. 11 Signal to Noise Ratio for LED versus distance from pipe exit non-dimensionalized by pipe diameter at 50 kfps for various exposure times.

Figure 10 shows that for tests using the HID source, the SNR corresponding to 10 µs exposures are considerably greater than the SNR corresponding to 1 µs exposures. This is due to the significantly greater amount of light collected by the camera in 10 µs compared to 1 µs. The x-axis represents the distance of the lead shock from the pipe exit (x) non-dimensionalized by the internal diameter of the pipe (D). Note that the framing rate for these tests corresponds to 50 kfps and the camera resolution was reduced to 960 x 80 pixels. Since the shock wave decreases in strength as it propagates away from the pipe exit, the SNR decreases at later frames.

For the LED, the data is shown in Figure 11. It can be seen that the 1 μs exposure provides a higher SNR than the 10 μs tests. The rate of decrease in the SNR is much larger for the LED tests in comparison to the HID tests. In addition to the decrease in shock wave strength, the depletion of the capacitors in the LED system contributes to the higher rate of decay in SNR.

6 Discussion

The results indicate that the relative performance of the HID and LED with regards to image quality is dynamic. In general, the LED outperforms the HID when operating over fewer frames and at shorter exposures. For example, side-by-side comparisons (Fig. 7) indicate that the image quality of the LED exceeds that of the HID at early times (t = 0.1 ms) at short exposures (1 μs). This is confirmed quantitatively in Figs. 10 and 11, where the SNR corresponding to LED tests (~50) is more than double the SNR corresponding to HID tests (~20) at early times. As per the ISO 12232 standards, the image quality of the lead shock wave is considered to be "excellent" for the LED and "good" for the HID. However, as the total number of pulses increase, the image quality becomes comparable. The SNR associated with both the HID and LED at t = 0.4 ms and 1 μs are roughly 20, indicating "good quality". Note that the decrease in LED performance is not inherent but due to the limited energy stored in the capacitors.

At longer exposures (10 μs) and increasing number of total frames, the SNR associated with the HID tests becomes larger in comparison to the LED tests (Figs. 10 and 11). For slower moving events, such as the jet shear layer, the camera sensor is able to integrate more light during the longer exposure, translating to a higher quality image (Fig. 7). As a consequence of the longer exposure, all of the faster moving events, such as the lead shock wave and interior compression waves become excessively blurred. Note that the LED system was designed to capture the high-speed flow structures and was not expected to perform well at long exposure times. In this experiment, the spherical shock wave is relatively weak, corresponding to a shock Mach number of 1.15 (396 m/s). The task of minimizing blur would become more challenging if faster events were to be imaged, such as a propagating detonation wave (~2000 m/s).

Several improvements to the LED system need to be implemented to image these faster events. First, the pulse duration needs to be further reduced to limit blur to the order of a few pixels. The circuit response shown in Fig. 2 indicates that the pulse duration can be reduced below 1 μs. Although the photodiode output shows a relatively long rise time of the LED response, the fall time is relatively short. By delaying the camera trigger relative to the trigger in, a process known as frame straddling, the camera sensor could be exposed to a sub microsecond duration of relatively high-intensity, uniform light. However, as the pulse duration decreases, it is expected that the SNR will also decrease. Although, higher current over-drive at these shorter pulse durations (Fig. 3) could compensate and maintain a high level of SNR. Other modifications, such as better matching between the LED spectral output and the spectral response of the CMOS camera sensor, could also improve SNR. Increasing the system capacitance is expected to extend the total number of bright pulses that can be achieved.

7 Conclusions

The novel LED system was shown to produce high-quality schlieren images of a weak, under-expanded helium jet. Direct image comparisons and signal-to-noise calculations between LED and HID light sources indicate that the over-driven LED system is more suited for fast-moving fluid dynamic events such as the imaging of low-amplitude compression waves and stronger shock waves. However, the HID was found to outperform the LED when imaging slower events such as the jet shear layer since longer exposure times could be used. At shorter pulse durations, the over-driven LED was able to produce higher intensity light compared to the continuous output of the HID. At longer pulse durations, the limited capacitance of the LED pulser restricted high performance to a relatively low number of pulses. A further advantage noted during testing is the reduced heat produced while operating the LED in comparison to the HID. It is expected that increasing capacitance of the LED system will extend the total number of pulses without degrading performance. Several modifications to the original Willert circuit allowed the pulse widths to be reduced, as well the maximum current increased without damaging the circuit. It is expected that the LED signal-to-noise ratio could be further improved and image blur reduced by decreasing the pulse width to the sub-microsecond rage while increasing the pulse current.

Acknowledgements
The private communications with Dr. Christian Willert, Dr. Ryan Bespalko and Dr. Gary Settles are gratefully acknowledged. Financial support for this work is from Dr. Johansen's Alberta Innovates Technology Futures (AITF) Strategic Chair position and equipment support from CMC Microsystems to Dr. Murari via the emSYSCAN program.

References

[1] T. Mizukaki, K. Wakabayashi, T. Matsumura and K. Nakayama, "Background-oriented schlieren with natural background for quantitative visualization of open-air explosions," *Shock Waves,* Vols. DOI 10.1007/s00193-013-0465-4 2013, 2013.

[2] G. Ciccarelli, C. Johansen and M. Kellenberger, "High-speed flames and DDT in very rough-walled channels," *Combustion and Flame,* vol. 160, no. 1, pp. 204-211, 2013.

[3] S. Saravanan, K. Nagashetty, G. Hedge, G. Jagadeesh and K. Reddy, "Schlieren visualization of shock wave phenomena over a missile-shaped body at hypersonic Mach numbers," in *Proceedings of the Institution of Mechanical Engineers, Part G., Journal of Aerospace Engineering*, 2011.

[4] A. Ben-Yakar and R.K.Hanson, "Ultra-fast-framing schlieren system for studies of the time evolution of jets in supersonic crossflows," *Experiments in Fluids,,* vol. 32, pp. 652-666, 2002.

[5] J. Gregg, *Personal Communication,* High Speed Imaging (HSI), November 25, 2013.

[6] C. Misiewicz, L. Myrabo, M. Shneider and Y. Raizer, "Combined Experimental and Numerical Investigation of Electric-Arc Airspikes for Blunt Body at Mach 3," in *35th AIAA Plasmadynamics and Lasers Conf.*, Portland, OR, 2004.

[7] G. Settles, T. Grumstrup, J. Miller, M. Hargather, L. Dodson and J. Gatto, "Full-scale high-speed 'Edgerton' retroflective shadowgraphy of explosions and gunshots," in *Proc. PSFVIP-5 5th Pacific Symp. Flow Visualization and Image Processing*, Austrailia, 2005.

[8] B. Zakharin, J. Stricker and G. Toker, "Laser-Induced Spark Schlieren Imaging," *AIAA Journal,* vol. 37, no. 9, pp. 1133-1135, 1999.

[9] D. Jonassen, G. Settles and M. Tronosky, "Schlieren "PIV" for turbulent flows," *Optics and Lasers in Engineering,* vol. 44, pp. 190-207, 2006.

[10] J. Shepherd, "Detonation in gases," *Procedings of the Combustion Institute,* vol. 32, pp. 83-98, 2009.

[11] D. Blumel, *Personal Communication,* XeVision, 2012.

[12] P. Rainbow, *Personal Communication,* Laser Components, 2012.

[13] Digi-Key Corporation, "Electronic Components Distributor | DigiKey Corp.," [Online]. Available: http://www.digikey.ca/. [Accessed May 2012].

[14] Mouser Electronics, Inc., "Mouser Electronics - Electronic Components Distributor," [Online]. Available: http://ca.mouser.com/. [Accessed May 2012].

[15] C. Willert, B. Stasicki, J. Klinner and S. Moessner, "Pulsed operation of high-power light emitting diodes for imaging flow velocimetry," *Measurement Science and Technology, vol. 21, No. 7, Jul/2010,* vol. 21, no. 7, 2010.

[16] C. Willert, D. Mitchell and J. Soria, "An assessment of high-power light-emitting diodes for high frame rate schlieren imaging," *Experiments in Fluids,* vol. 53, no. 2, pp. 413-421, 2012.

[17] M. Biss, G. Settles, M. Hargather, L. Dodson and J. Miller, "High-speed digital shadowgraphy of shock," in *Shock Waves*, Berlin, Springer, 2009, pp. 91-96.

[18] C. Willert, *Personal Communication,* 2012.

[19] R. Bespalko, *Personal Communication,* 2012.

[20] N. Buchmann, C. Willert and J. Soria, "Pulsed, high-power LED illumination for tomographic particle image velocimetry," *Experiments in Fluids,* vol. 53, no. 5, pp. 1545-1560, 2012.

[21] Texas Instruments, "Single 9-A High Speed Low-Side MOSFET Driver with Enable Datasheet," Dallas, TX, 2004.

[22] G. Settles, Schlieren and shadowgraph techniques, Berlin: Springer, 2001.

[23] International Organization for Standardization, "ISO 12232:2006 -- Photography -- Digital still cameras -- Determination of exposure index, ISO speed ratings, standard output sensitivity, and recommended exposure index," 2006.